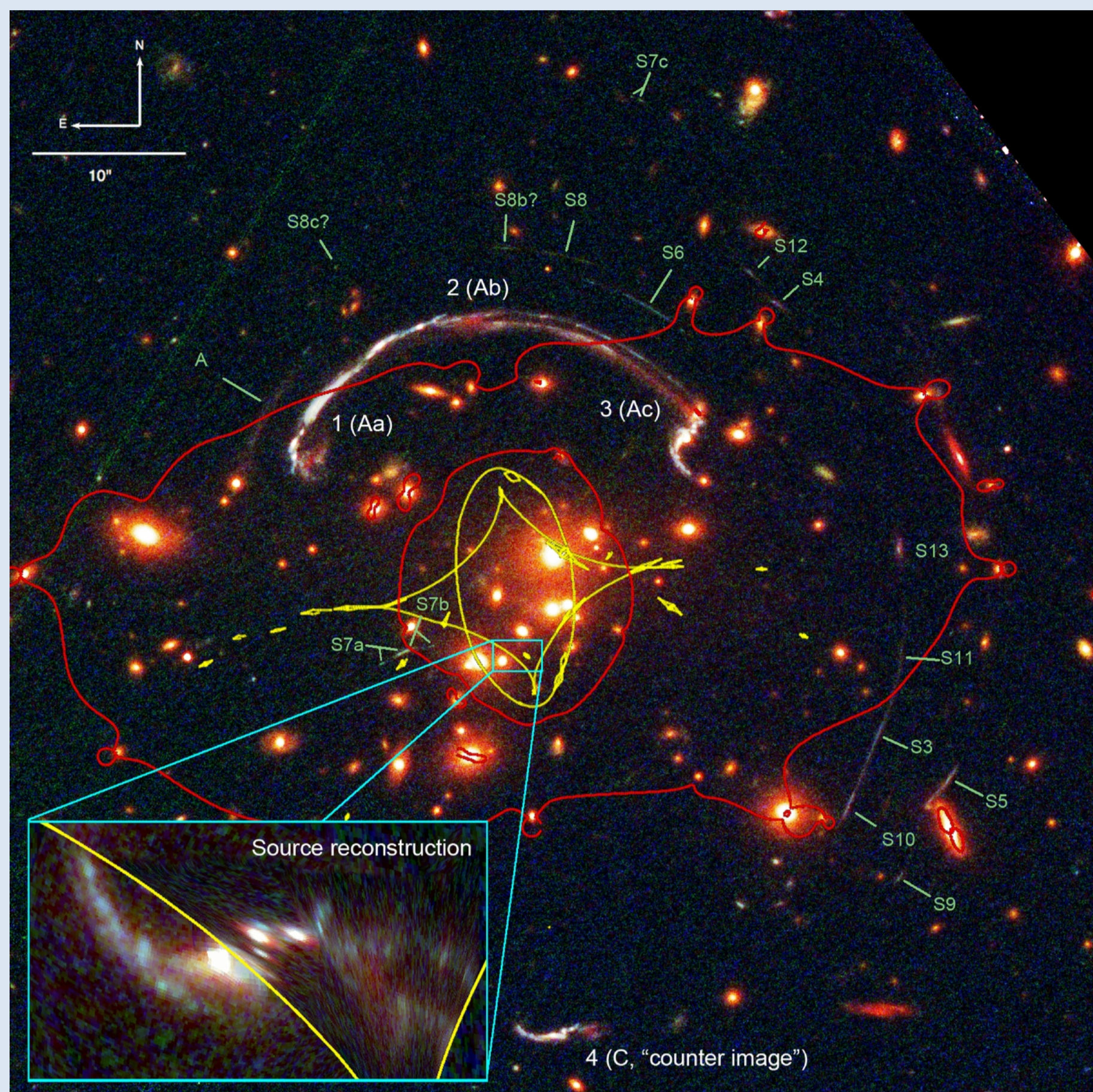




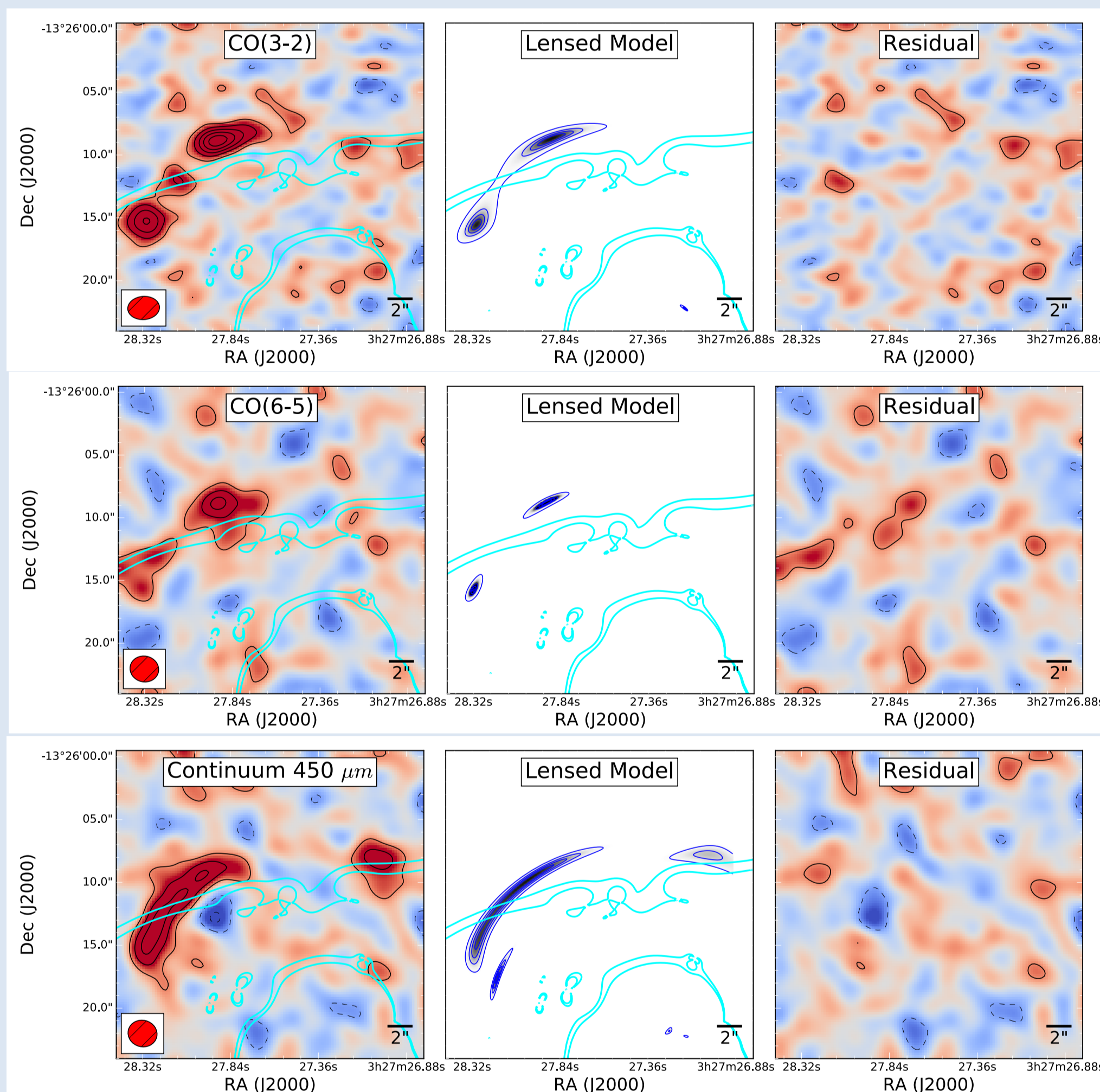
L. Felipe Barrientos, J. Gonzalez, et al



The Target

The arc RCGS0327-132609 is the second brightest optical giant arc known (Wuyts et al 2010). The system consists of a giant arc that extends over $38''$ on the sky and is made up of three merged images of the background source at $z=1.7$. There is also a bright counter image at the opposite side of the cluster. The total magnification is about 30. The source intrinsic stellar mass is $6.3 \pm 0.7 \times 10^9 M_{\odot}$ and SFR of $30\text{--}50 M_{\odot} \text{ yr}^{-1}$ (Wuyts et al. 2012) translate into a specific SFR $\log(\text{sSFR } \text{yr}^{-1}) = -8.3$. The lensing cluster is at $z=0.56$ with a velocity dispersion of $1139 \pm 19 \text{ km/s}$.

The kinematic analysis of H α on RCGS0327-132609 strongly suggest an interaction consistent with a merger of galaxies (Wuyts 2014). The SFRs measured in individual clumps and across the galaxy fall well above the MS relation for galaxies at $z=1.7$ and are consistent with a young low-metallicity ($\sim 0.3 Z_{\odot}$) starburst enhanced by the ongoing merger (Wuyts 2014, Whitaker 2014). In addition, Bordoloi (2016) measured resolved galactic winds on RCGS0327, showing that the outflows are comparable to those observed in local starbursts. In summary, RCGS0327 presents several characteristics that can be associated to high redshift SMGs, while presenting an SFR $\sim 30\text{--}50 M_{\odot} \text{ yr}^{-1}$ in the range of color selected galaxies (CSGs) at high redshift.

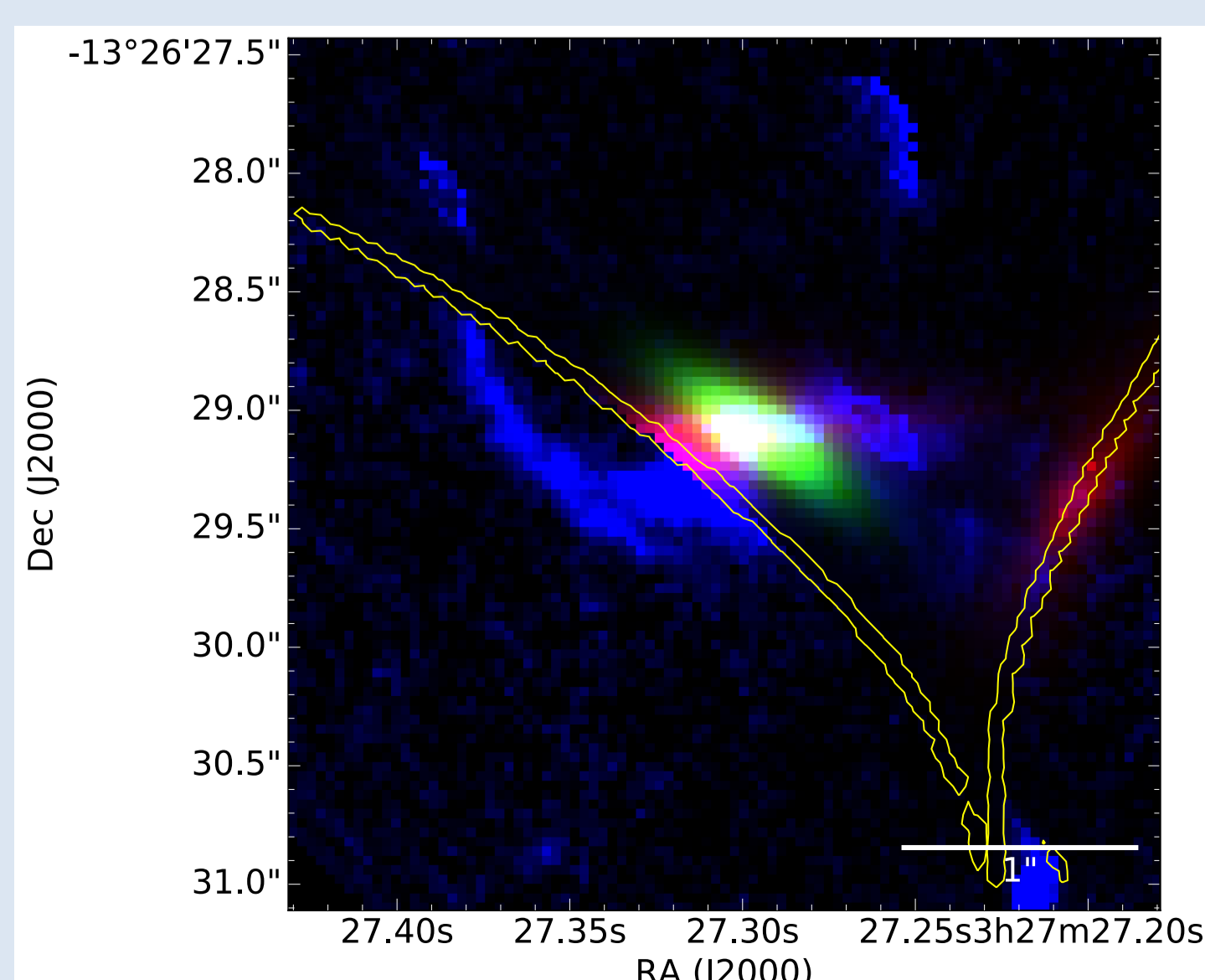


Models

To model the emission from RCGS0327-132609 we used the mass model produced by Sharon et al (2012) and a modified version of *uvmmcmfit* (Bussmann et al 2013, Bussmann et al 2015, Gonzalez-Lopez et al 2017) in which the potential is known. The source emission is modeled by a 2D elliptical Gaussian distribution which is then lensed to the image plane using the provided deflection fields. The visibilities are simulated and compared to the observed ones. This process is repeated until the fit model converges and the observed and simulated visibilities agree (within the uncertainties). The best fitted model in the image plane are shown in the figure above.

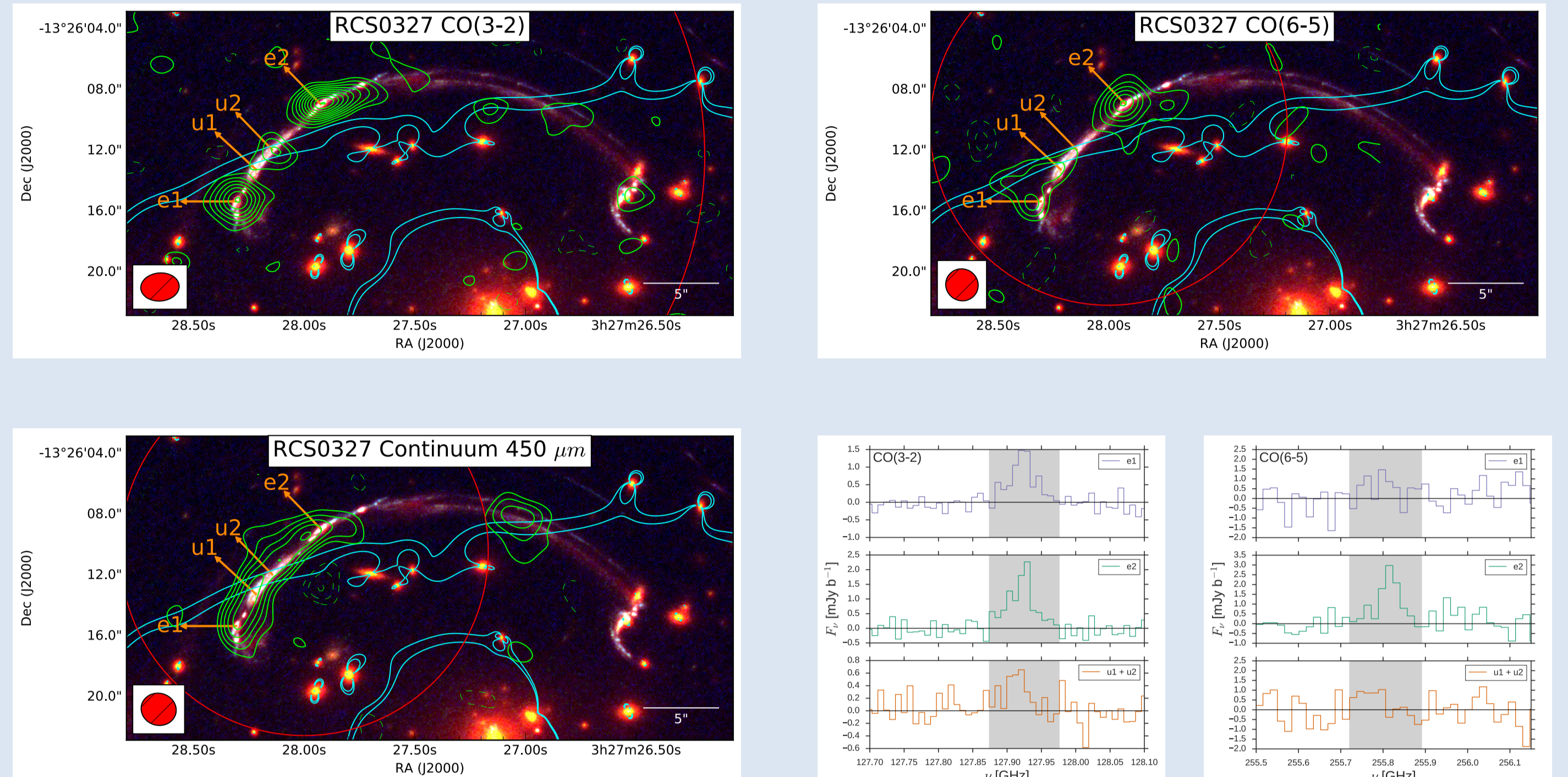
The CO(3-2) was well fitted by a single 2D elliptical Gaussian having an intrinsic flux of $S_{\text{CO}(3-2)} = 70.5 \pm 6 \mu\text{Jy}$ (for the frequency range of 240 km s^{-1}), effective radius $r_s = 0.142 \pm 0.025 \text{ arcsecs}$. In the case of CO(6-5), with a single component we obtain $S_{\text{CO}(6-5)} = 77.7 \pm 13 \mu\text{Jy}$ and an effective radius $r_s = 0.055 \pm 0.020 \text{ arcsecs}$. To fit the continuum emission at $450 \mu\text{m}$, we needed two Gaussians in the source plane. The main component is well described with $S_{450} = 48.1_{-16.6}^{+54.9} \mu\text{Jy}$ and $r_s = 0.211 \pm 0.050 \text{ arcsecs}$. The second component has $S_{450\mu\text{m}} = 25.5_{-12.5} \mu\text{Jy}$ and $r_s = 0.17 \pm 0.10 \text{ arcsecs}$. With this model the intrinsic CO(3-2) luminosity is $L'_{\text{CO}(3-2)} = 2.90 \pm 0.21 \times 10^8 \text{ K km s}^{-1} \text{ pc}^2$, for CO(6-5) is $L'_{\text{CO}(6-5)} = 8.0 \pm 1.3 \times 10^7 \text{ K km s}^{-1} \text{ pc}^2$.

The bottom panel shows a composite of the different observed emission of RCGS0327 in the source plane. The blue channel represents the delensed F814W emission, the green channel corresponds to the CO(3-2) emission and the red channel corresponds to the continuum emission at $450 \mu\text{m}$. The CO(3-2) and continuum emission come mainly from the clumps labeled as a to f in Sharon et al (2012) and Wuyts et al (2014). The cyan and blue solid lines represent the caustic curves in the source plane.



Abstract

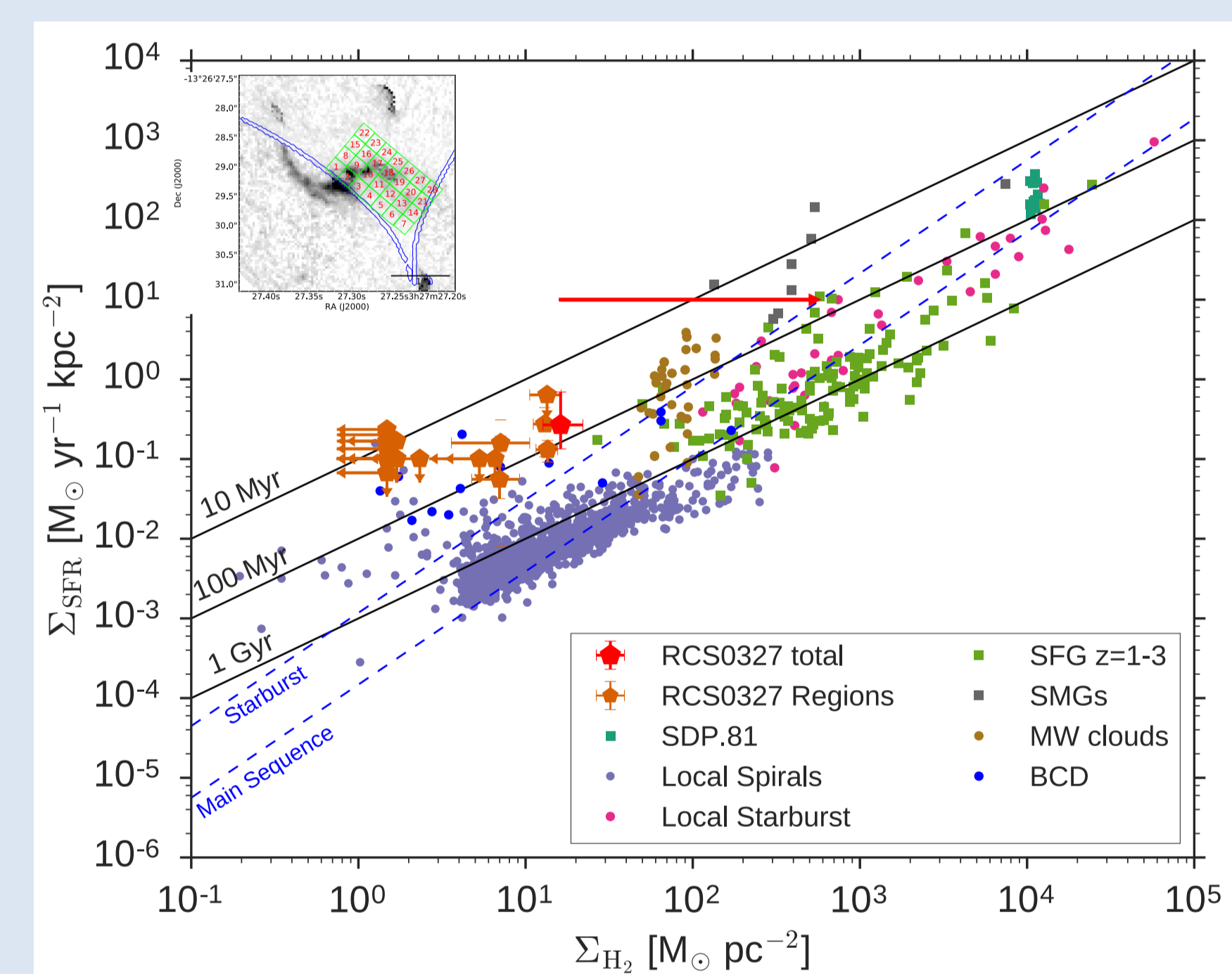
We present Atacama Large Millimeter/submillimeter Array observations of CO lines and dust continuum emission on the source RCGS0327-132609, a young $z=1.7$ low-metallicity starburst galaxy. The CO(3-2), CO(6-5) lines and continuum at rest-frame 450 m are detected with high significance and show a resolved structure in the image plane. We used the corresponding lensing model to obtain a source plane reconstruction of the detected emission. The intrinsic properties of RCGS0327-132609 show an enhanced star-formation activity compared to local spiral galaxies with similar molecular gas densities, supporting the starburst phase scenario.



Observations

RCGS0327-132609 was observed as part of the ALMA project 2015.1.00920.S which consisted of observations of the emission lines CO(3-2), CO(6-5) and CO(8-7) and the underlying continuum at the corresponding frequencies. At the best redshift estimate for RCGS0327 of $z=1.7037455$, the lines are centered at 127.895 GHz in ALMA band 4 for CO(3-2), 255.746 GHz in ALMA band 6 for CO(6-5) and at 340.934 GHz in ALMA band 7 for CO(8-7). The observations of the lines CO(6-5) and CO(3-2) were carried out during January 1st and the 10th of 2016. The observations of CO(8-7) were unfortunately not completed during the cycle 3. Both emission lines were observed using the array configuration C36-1. The imaging of the calibrated data was done using the casa task **clean**. The final imaging has a resolution of about $2''$.

In a 240 km s^{-1} window (shown in the panel above) we find the total arc integrated flux for CO(3-2) is $0.904 \pm 0.159 \text{ Jy km s}^{-1}$, and for CO(6-5) is $0.883 \pm 0.525 \text{ Jy km s}^{-1}$. The spatially integrated continuum emissions measured in the same region as CO(3-2) are $S_{450\mu\text{m}} = 960 \pm 98 \mu\text{Jy}$ and $S_{875\mu\text{m}} = 141 \pm 31 \mu\text{Jy}$.



Results

We use the CO(3-2) to estimate the amount and distribution of molecular gas in the galaxy. We assume a CO excitation level valid for SMGs of $L'_{\text{CO}(3-2)}/L'_{\text{CO}(1-0)} = 0.66$ to obtain an intrinsic CO line luminosity of $L'_{\text{CO}(1-0)} = 4.40 \pm 0.35 \times 10^8 \text{ K km s}^{-1} \text{ pc}^2$ and $\text{H}_2 = 3.51 \pm 0.26 \times 10^8 M_{\odot}$, using a CO conversion factor of $\alpha_{\text{CO}} = 0.8 \text{ (K km s}^{-1} \text{ pc}^2)^{-1}$. With the effective radius measured for the CO(3-2) emission we estimate the total area for the molecular gas surface of $A_{\text{CO}(3-2)} = 21.7 \pm 5.6 \text{ kpc}^2$ and obtained a H_2 surface density of $\Sigma_{\text{H}_2} = 16.2 \pm 5.8 M_{\odot} \text{ pc}^{-2}$. With the measured size for the continuum emission in the source plane and an estimate of the SFR from the optical, we obtain a surface density of SFR $\Sigma_{\text{SFR}} = 0.27^{+0.43}_{-0.13} M_{\odot} \text{ yr}^{-1} \text{ kpc}^{-2}$.

We also derived resolved properties for individual regions marked in the inset in the Figure above, where we also present the resolved properties for the total emission of RCGS0327 and for each of the individual regions. We compared the results with those from the literature for a wide range of populations. RCGS0327 clearly falls above the relation found by Daddi et al. (2010) for MS and starburst galaxies (blue dashed-lines), supporting the starburst nature of RCGS0327.

Assuming that our molecular mass estimate is accurate, we see that RCGS0327 properties are similar to the local BCDs, which are low-metallicity starburst galaxies that show higher star forming efficiencies when compared to normal disc galaxies.

We have shown that even with coarse ALMA observations we are able to resolved the ISM in a starburst galaxy at the peak of the star-formation activity in the Universe.

References

- Bordoloi R., Rigby J. R., Tumlinson J., Bayliss M. B., Sharon K., Gladders M. G., Wuyts E., 2016, MNRAS 458, 1891
- Bussmann, R. S., Perez-Fourmon, I., Amber, S., et al. 2013, ApJ, 779, 25 (B13)
- Bussmann, R. S., Riechers, D., Fialkov, A., et al. 2015, ApJ, 812, 43
- Daddi, E., Elbaz, D., Walter, F., et al. 2010, ApJL, 714, L118
- Gonzalez-Lopez, J., Bauer, F. E., Romero-Cañizales, C., et al. 2017, A&A, 597, A41
- Sharon K., Gladders M. D., Rigby J. R., Wuyts E., Koester B. P., Bayliss M. B., Barrientos L. F., 2012, ApJ 746, 161
- Whitaker K. E., Rigby J. R., Brammer G. B., Gladders M. D., Sharon K., Teng S. H., Wuyts E., 2014, ApJ 790, 143
- Wuyts E., Barrientos L. F., Gladders M. D., Sharon K., Bayliss M. B., Carrasco M., et al., 2010, ApJ 724, 1182
- Wuyts E., Rigby J. R., Sharon K., Gladders M. D., 2012, ApJ 755, 73
- Wuyts, E., Rigby, J. R., Gladders, M. D., & Sharon, K. 2014, ApJ, 781, 61